



## Full length article

# EsGPCR89 regulates cerebral antimicrobial peptides through hemocytes in *Eriocheir sinensis*

Xiang Qin<sup>a</sup>, Xingkun Jin<sup>b</sup>, Kaimin Zhou<sup>a</sup>, Hao Li<sup>a</sup>, Qiyang Wang<sup>a</sup>, Weiwei Li<sup>a,\*</sup>, Qun Wang<sup>a,\*\*</sup>

<sup>a</sup> State Key Laboratory of Estuarine and Coastal Research, and The Laboratory of Invertebrate Immunological Defense and Reproductive Biology, School of Life Science, East China Normal University, Shanghai, PR China

<sup>b</sup> Department of Marine Biology, College of Oceanography, Hohai University, Nanjing, PR China

## ARTICLE INFO

## Keywords:

*Eriocheir sinensis*  
GPCRs  
Cerebral immunity  
Antimicrobial peptides

## ABSTRACT

G protein-coupled receptors (GPCRs) are important transmembrane receptors that participate in diverse physiological processes including metabolism, cell growth and immune processes by transmitting extracellular signals to intracellular effectors. In this study, a gene belonging to the GPCR family was cloned from *Eriocheir sinensis* and named *EsGPCR89*. The full-length gene includes an open reading frame (ORF) of 465 amino acid residues, and bioinformatic analysis confirmed the high conservation between species. *EsGPCR89* was detected in various tissues of *E. sinensis*, and was up-regulated in brain following *Staphylococcus aureus* infection. Expression levels of cerebral antimicrobial peptides (AMPs) were also up-regulated following bacterial challenge, reflecting their function in cerebral immunity. Additionally, *EsGPCR89* silencing in hemocytes by RNA interference, down-regulated AMPs in brain after *S. aureus* infection. Moreover, through Immunisation assay and Polyacrylamide gel electrophoresis (SDS-PAGE) experiments, we could infer that bacterially infected hemocytes released effectors under the regulation of *EsGPCR89*, thereby activating transcription of cerebral AMPs. These results demonstrate that *EsGPCR89* plays important roles in cerebral antimicrobial function via hemocytes.

## 1. Introduction

Animals are constantly threatened by invasion of pathogens, and have evolved immune systems to eliminate infectious microorganisms [1]. The immune system of gnathostomes consists of two branches; innate and acquired immunity [2,3]. In invertebrates, although some studies have revealed an alternative adaptive immune system in arthropods [4,5], innate immunity still plays a significant role in blocking microbial invaders. The innate immune system recognises pathogen-associated molecular patterns (PAMPs) absent in the host body but present on the surface of microorganisms, such as lipopolysaccharides (LPS), peptidoglycans and  $\beta$ -1,3-glucans, through germline-encoded pattern recognition receptors (PRRs) [6]. In *Drosophila*, recognition of PAMPs leads to both cellular and humoral reactions. These cellular responses include hemocyte phagocytosis, encapsulation, and degranulation, leading to local release of antibiotic substances. Compared with its counterparts, humoral responses include prophenoloxidase (proPO) activity, coagulation cascades, and release of AMPs through Toll, IMD and Jak-STAT intracellular signalling pathways [7–10]. AMPs are vital components of immune systems in invertebrates that act

against bacteria, fungi, protozoa and viruses, and they also mediate innate immunity [11].

In vertebrates, the central nervous system (CNS) is generally considered to be immuno-privileged [12]. Due to its importance, the CNS might affect the ability to fight infections by providing an environment conducive to innate immune responses [13]. Additionally, regulation of innate immune responses in the brain might be associated with Toll-like receptors (TLRs) [14]. In recent years, G protein-coupled receptors widely involved in both innate and adaptive immunity in mammals have been discovered to be important signal mediators. However, the immune function of GPCRs in invertebrates remains poorly understood.

G protein-coupled receptors (GPCRs) are the most diverse family of cell surface receptors. More than 50% of prescription drugs target GPCR-mediated signalling pathways, emphasising their importance in human disease [15]. The GPCR superfamily comprises > 800 distinct human proteins sharing a common seven transmembrane (7TM)  $\alpha$ -helical fold [16]. Three extracellular loops (ECL1–3) and three intracellular loops (ICL1–3) connect the 7TM bundle [17]. GPCRs are transmembrane receptors that transmit external signals to intracellular effectors by binding extracellular ligands, thereby participating in a

\* Corresponding author.

\*\* Corresponding author.

E-mail addresses: [wqli@bio.ecnu.edu.cn](mailto:wqli@bio.ecnu.edu.cn) (W. Li), [qwang@bio.ecnu.edu.cn](mailto:qwang@bio.ecnu.edu.cn) (Q. Wang).

<https://doi.org/10.1016/j.fsi.2019.10.015>

Received 27 June 2019; Received in revised form 2 September 2019; Accepted 7 October 2019

Available online 09 October 2019

1050-4648/© 2019 Elsevier Ltd. All rights reserved.

variety of physiological processes [18] such as cellular metabolism [19], secretion, neurotransmission [20–22], cellular differentiation and growth, and pathological conditions including inflammation and immunoreaction [23]. Compared with the extensive literature relating GPCRs to vertebrate immunity, their immune functions in invertebrates are poorly studied. Some GPCRs in mammals such as chemokine receptors are involved in immune responses [24]. However, evidences for the role of GPCRs in immune processes in invertebrates remains insufficient.

Due to the molecular architecture of GPCRs, which are particularly suitable for binding diverse chemical structures [25], and the evolutionary relationships among mammals [26], GPCRs may perform specific functions in innate immune processes in invertebrates. The first indication of the role of GPCRs in immune defence came from studies on horseshoe crabs (*Limulus polyphemus*) in which blood undergoes rapid coagulation after exposure to Gram-negative bacterial pathogens [27]. By analogy with activation of GPCRs, it is inferred that there was an as-yet-undiscovered GPCR giving rise to diverse intracellular responses [28]. In *Caenorhabditis elegans*, a GPCR named *F5HR-1* (Follicle-stimulating Hormone Receptor) possessing a leucine-rich repeat (LRR) domain might act as a pathogen receptor in the intestines [29] and a GPCR named *NPR-1* (Neuropeptide Receptor) involved in neural circuit function suppresses innate immune responses. In addition, a putative GPCR in red swamp crayfish named *HPIR* (a Protein Receptor in Hepatopancreas) is up-regulated in hepatopancreas following challenge with heat-killed *Aeromonas hydrophila*, indicating a role in the defence against bacterial infection [30]. A GPCR serotonin receptor named *5-HTTR-1* in *Crassostrea gigas* is up-regulated after simulation by LPS, indicating an immune role for this novel member of the *5-HT1* receptor family [31]. As for the neuro-immune studies that are relevant to our work, results on serotonin (*5-HT*) in the brain provided new targets for drug development in major depression [32]. Other than this, a GPCR named *Moody* was identified to be related to the formation of blood-brain barrier (BBB) in *Drosophila* [33]. In mammals, this BBB not only protects the brain from pathogen, toxic molecules and damage of the autoimmune system, but also is important for brain homeostasis [34].

Chinese mitten crab (*Eriocheir sinensis*) is one of the most economically important aquaculture species in China and elsewhere in Asia. This species is threatened by numerous pathogens, making the study of its immune defences particularly important. In the present work, we identified a new GPCR gene in *E. sinensis* (*EsGPCR89*). The full-length cDNA was obtained and analysed by bioinformatics. *In vivo* bacterial infection experiments and interference assays were performed, immune functions and regulation were preliminarily explored, and the effect of AMP expression in the brain was investigated. The results demonstrate a clear role in immune defences, and provide insight on interactions between immune and nervous systems in Chinese mitten crab.

## 2. Materials and methods

### 2.1. Experimental animals

Healthy Chinese mitten crabs ( $90 \pm 10$  g wet weight) were obtained from a local agricultural market in Shanghai, China. All crabs were maintained for a week under constant temperature (20–25 °C) in the Biology Station after transportation. Filtered and aerated freshwater was used to acclimate crabs and feeding was performed regularly to ensure a stable state before starting the experiment. Three independent repeats were performed in each experiment ( $\geq 5$  crabs per sample).

All animal experiments were performed according to the protocol approved by the Ethics Committee of Laboratory Animal Experimentation at East China Normal University and Use Committee (Protocol license number: AR2012/12017). Experiments were conducted in accordance with the guidelines on animal care of the Ministry of Science and Technology of the People's Republic of China.

### 2.2. Immune challenge and sample collection

*S. aureus* (BYK0113) was obtained from the National Pathogen Collection Center for Aquatic Animals (Shanghai Ocean University, Shanghai, China), since this organism is the major pathogen causing serious disease in the aquaculture industry [35]. Bacteria were collected by centrifugation at  $5000 \times g$  for 5 min after culturing for 12 h overnight in Luria Bertani (LB) medium. After washing three times using sterile phosphate-buffered saline (PBS; 137 mM NaCl, 2.7 mM KCl, 10 mM  $\text{Na}_2\text{HPO}_4$ , 2 mM  $\text{KH}_2\text{PO}_4$ , pH 7.4) and resuspending the cell pellet, colony-forming units (CFU) were counted using the serial dilution method.

Healthy and viable Chinese mitten crab were selected for *in vivo* bacterial infection experiments. All crabs were randomly divided into two groups; *S. aureus*-infected and non-infected controls. After overnight culturing, *S. aureus* cells were washed with PBS and diluted to  $1 \times 10^8$  CFU/ml, and 100  $\mu\text{l}$  was injected into the hemolymph at the membrane of the third walking leg (100  $\mu\text{l}$  of PBS was injected into controls). Brains were sampled at 0, 2, 6, 12, 24 and 48 h after injection from more than three crabs for each timepoint. Hemolymph (5 ml per crab) was extracted from posterior walking legs using a sterile syringe containing 5 ml anticoagulation solution (0.14 M NaCl, 0.1 M glucose, 30 mM trisodium citrate, 26 mM citric acid, 10 mM EDTA, pH 4.6) [36] and centrifuged to pellet the hemocytes. All samples were stored at  $-80$  °C. Heart, brain, gill, muscle, intestine, stomach, hepatopancreas and hemocyte samples were also obtained from healthy untreated (control) crabs.

### 2.3. Total RNA extraction and cDNA synthesis

Total RNA from hemocytes and tissues were extracted using a MagMAX mirVANA Total RNA Isolation Kit (ThermoFisher Scientific, USA) and TRIzol Reagent (Invitrogen, USA) according to the manufacturer's instructions. RNA concentration and purity were measured using a NanoDrop 2000 spectrophotometer (Thermo Fisher Scientific). The quality of RNA was assessed by 1% agarose gel electrophoresis (AGE). First-strand cDNA used for gene cloning was obtained using a PrimeScript 1st Strand cDNA Synthesis Kit (TaKaRa, Japan) according to the manufacturer's instructions, and cDNA used for quantitative real-time PCR (qRT-PCR) was obtained from total RNA (4  $\mu\text{g}$ ) by reverse transcription using a PrimeScript RT reagent Kit with gDNA Eraser (Perfect Real Time; TaKaRa).

### 2.4. Cloning of the *EsGPCR89* gene

In order to obtain the full-length *EsGPCR89* gene, 5  $\mu\text{g}$  of total RNA was reverse-transcribed using a SMARTer RACE 5'/3' Kit (Clontech, Japan) following the manufacturer's protocol. The expressed sequence tag (EST) of *EsGPCR89* was searched against the hemocyte cDNA library of Chinese mitten crab (unpublished), and full-length *EsGPCR89* was amplified the partial gene according to the instructions supplied with the SMARTer RACE cDNA Amplification kit (Clontech, Shiga, Japan). Gene-specific primers (Table 1) based on the crab EST were designed by Rui Mian Company (Shanghai, China). PCR amplification included an initial denaturation at 94 °C for 4 min, followed by 32 cycles of denaturation at 94 °C for 30 s, annealing at 59 °C for 30 s, extension at 72 °C for 2 min, and a final extension at 72 °C for 7 min. All PCR products were assessed by AGE and the target gene was excised from the gel and purified using an Agarose Gel DNA Extraction Kit Ver.4.0 (TaKaRa). PCR products were inserted into the pEASY-T1 vector (TransGen, China), confirmed by DNA sequencing, and the full-length cDNA sequence of *EsGPCR89* was uploaded to GeneBank under accession number MN057664.

**Table 1**  
Primer sequences used for EsGPCR89 analysis.

Primer name	Sequence (5'-3')
<b>cDNA cloning</b>	
3'Ou-EsGPCR89	CAGTGTACTTCCAGCAGCCCTCA
3'In-EsGPCR89	GCTGTCCACTGGCTTGGCTTTGA
5'Ou-EsGPCR89	CCCTTGGTACTGGGCTTCTTCT
5'In-EsGPCR89	ATGTGACCTTTCTCGTTGTGCC
<b>Real-time quantitative PCR</b>	
β-actin qF	GCATCCACGAGACCACTTACA
β-actin qR	CTCTGCTTGTGATCCACATC
EsGPCR89 qF	TGATGCTGATGAGGATGAA
EsGPCR89 qR	AGAGGTGTGACTTGTCTT
EsDWD1 qF	ACGGGTCGTCAACGAAACTG
EsDWD1 qR	GGTCACTGGGTTACCATAGCG
EsALF1 qF	GACGCAGGAGGATGCTAAC
EsALF1 qR	TGATGGCAGATGAAGACAC
EsALF2 qF	GACCCTTTGCTGAATGCTTGA
EsALF2 qR	CTGCTCTACAATGTCGCCTGA
EsALF3 qF	ACGAGGAGCAAGGAAAGAAAG
EsALF3 qR	TTGTGCCATAGACCAGAGACTT
EsCrus1 qF	GCTCTATGGCGGAGGATGTCA
EsCrus1 qR	CGGGCTTCAGACCACTTTAC
EsCrus2 qF	GCCCACTCCAAAACCTAT
EsCrus2 qR	GCAAGCGTCACAGCAGCACT
EsLys qF	CTGGATGATGTGGAGAAGTGC
EsLys qR	TTATTCGGTGTGTTATGAGGGGT
<b>RNA interference</b>	
T <sub>7</sub> -EsGPCR89-F	TAATACGACTCACTATAGGGTGGCACAACGAGAAAGGGTC
T <sub>7</sub> -EsGPCR89-R	TAATACGACTCACTATAGGGACGGTGGTAGAAATGGAAGCTGC
T <sub>7</sub> -GFP-F	TAATACGACTCACTATAGGGACCTTATGATGCCGTTCTCTG
T <sub>7</sub> -GFP-R	TAATACGACTCACTATAGGGCCACAAGTTCACGGTGTCC

2.5. Bioinformatics analysis

The online search tool BLASTX (<http://www.ncbi.nlm.nih.gov/>) was used to compare the obtained sequence with homologs from other species in the NCBI (National Center for Biotechnology Information) database, and open reading frames (ORFs) were identified by ORF Finder (<http://www.ncbi.nlm.nih.gov/gorf/orf.cgi>). Structural and functional domains were predicted by SMART (<http://smart.embl-heidelberg.de/>) and transmembrane regions were identified by TMHMM Server v.2.0 (<http://www.cbs.dtu.dk/services/TMHMM/>). ClustalX 2.0 and BioEdit software were used to perform multiple sequence alignment, and evolutionary relationships between EsGPCR89 and other species were analysed by constructing a neighbour-joining (NJ) phylogenetic tree with 1000 replicates using MEGA 7.0 software.

2.6. Quantitative real-time PCR (qRT-PCR)

2.6.1. Tissue-specific expression

Total RNA was extracted from different tissues and cDNA was obtained. Specific primers for EsGPCR89 (EsGPCR89 qF and EsGPCR89 qR; Table 1) and β-actin (β-actin qF and β-actin qR; Table 1) were designed by Rui Mian Company. The tissue-specific expression pattern of EsGPCR89 was revealed by qRT-PCR analysis using SYBR Premix Ex TaqII (Ti RNaseH Plus; TaKaRa) and Applied Biosystems QuantStudio 3 & 5 (Thermo Fisher Scientific). β-actin served as a control housekeeping gene. Reactions were performed at 95 °C for 30 s, followed by 39 cycles at 95 °C for 5 s and 58 °C for 30 s. Data were analysed by QuantStudio Design & Analysis Software and relative expression values were

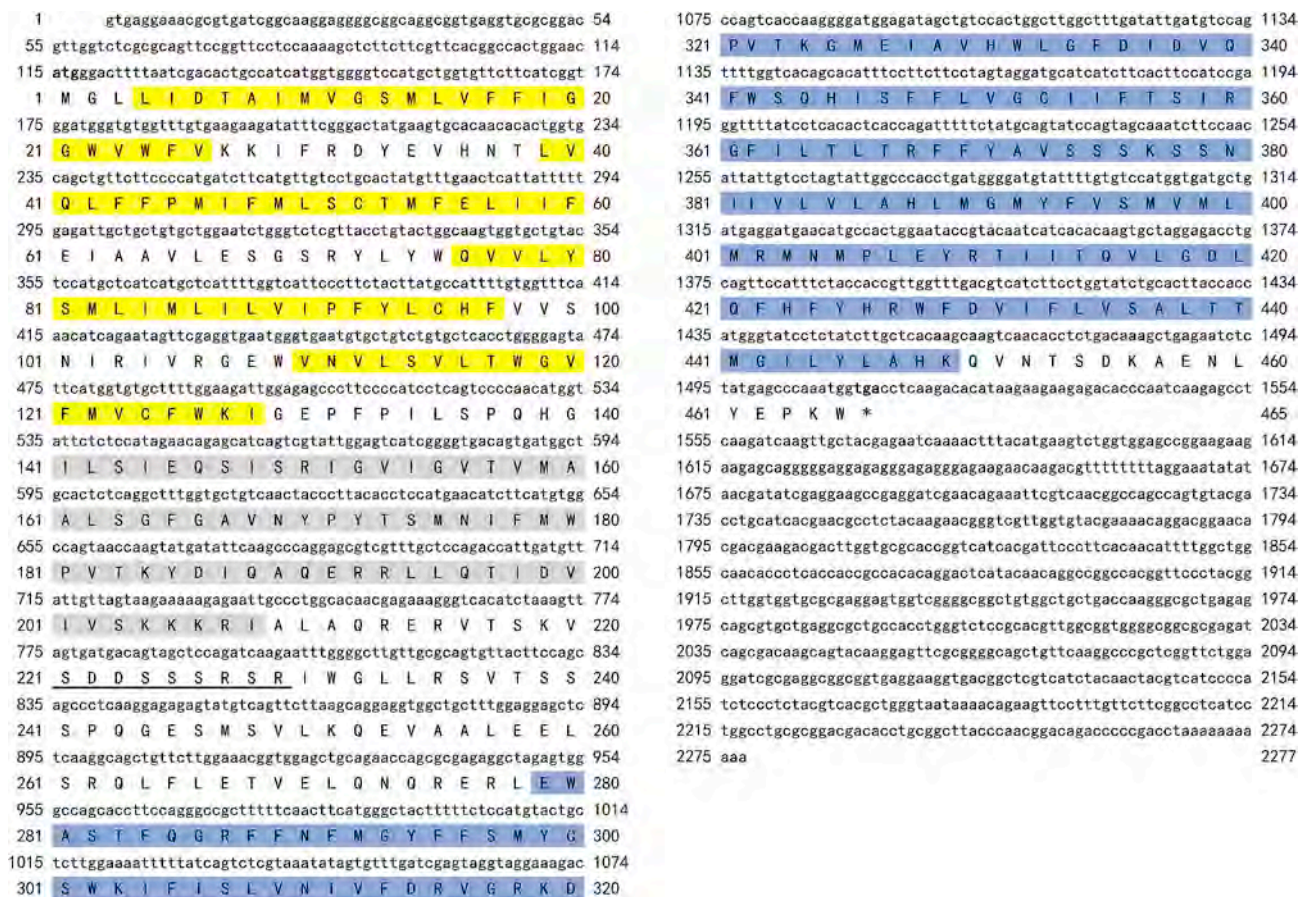


**Fig. 1.** Nucleotide and deduced amino acid sequences of EsGPCR89. Amino acid sequences are shown under the corresponding cDNA sequence. Transmembrane regions are shaded yellow, the GPHR\_N domain is shaded grey, and the ABA\_GPCR is shaded blue. The low-complexity region is underlined, and letters representing the initiation codon (ATG), terminal codon (TGA) is in bold. For interpretation of references to colour in this figure legend, the reader is referred to the online version of this article. (For interpretation of the references to colour in this figure legend, the reader is referred to the Web version of this article.)

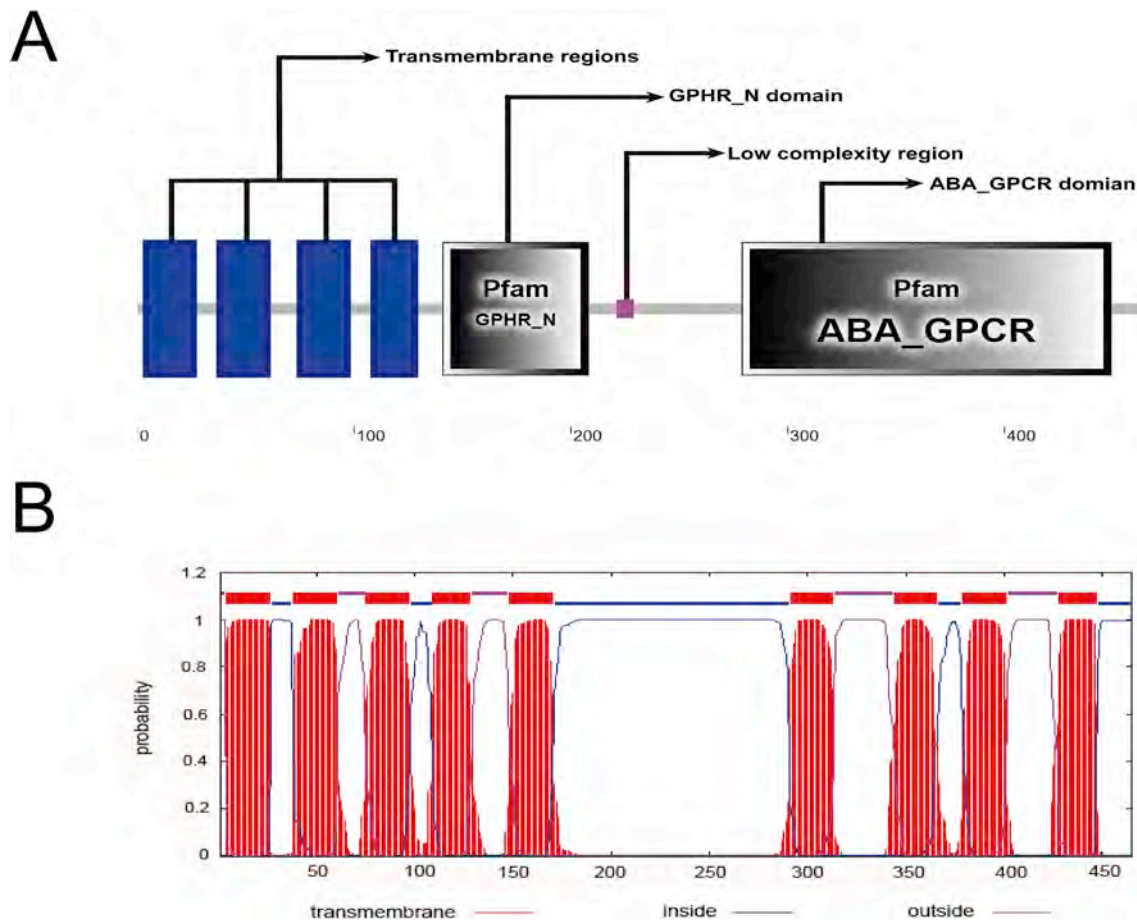


**Fig. 2.** Schematic diagram of the structure of the *EsGPCR89* protein. (A) Domain structure analysis of the putative *EsGPCR89* protein by SMART, indicating four transmembrane regions, a GPCR\_N domain, a low-complexity region and an ABA\_GPCR domain. (B) Prediction of transmembrane regions by the TMHMM server. Nine transmembrane domains are depicted as red lines. (For interpretation of the references to colour in this figure legend, the reader is referred to the Web version of this article.)

calculated using the comparative CT ( $2^{-\Delta\Delta C_t}$ ) method [37] based on Ct values for *EsGPCR89* and  $\beta$ -actin. Experiments were repeated three times for each sample, and data were analysed by one-way analysis of variance (ANOVA) and post-hoc Duncan's multiple range tests.

#### 2.6.2. Expression levels of *EsGPCR89* in brain

Relative expression levels of *EsGPCR89* in crab brain after infection with *S. aureus* were analysed by qRT-PCR. Total RNA (4  $\mu$ g) was used to prepare cDNA, and gene-specific primers were synthesised based on the cDNA sequence. Three independent replicates were included, and expression was normalised against  $\beta$ -actin. The reaction conditions and analytical method are described in 2.6.1.

#### 2.7. *EsGPCR89* RNA interference (RNAi) in vivo

##### 2.7.1. Preparation of double-stranded RNA (dsRNA)

Gene interference of GPCR89 was performed using dsRNA as described previously [38] with simple modification. Briefly, dsRNA was produced using a TranscriptAid T<sub>7</sub> High Yield Transcription Kit (Thermo Scientific) with a T<sub>7</sub> promoter-linked PCR product as template. For preparing templates, T<sub>7</sub> promoter-linked primers (T<sub>7</sub>*EsGPCR89*-F and T<sub>7</sub>*EsGPCR89*-R; Table 1) were synthesised and used to amplify an *EsGPCR89* fragment from cDNA. PCR products were collected and purified using an Agarose Gel DNA Extraction Kit Ver.4.0 (TaKaRa). Transcription reagents consisting of 4  $\mu$ l of 5  $\times$  TranscriptAid Reaction Buffer, 8  $\mu$ l of NTP mix, 1  $\mu$ g of template DNA, 2  $\mu$ l of TranscriptAid

Enzyme Mix, and DEPC-treated water to 20  $\mu$ l were mixed and incubated at 37  $^{\circ}$ C for 2 h. Residual template DNA was removed by adding 2  $\mu$ l of DNase I (RNase-free) and incubating at 37  $^{\circ}$ C for 15 min. Next, 2  $\mu$ l of 0.5 M EDTA (pH 8.0) and placed at 65  $^{\circ}$ C for 10 min. For RNA transcript purification, 115  $\mu$ l of DEPC-treated water and 15  $\mu$ l of 3 M sodium acetate solution (pH 5.2) were added and RNA was extracted by chloroform and precipitated by ethanol. After rinsing the RNA pellet with 70% ethanol, RNA was resuspended in DEPC-treated water and subjected to electrophoresis for RNA integrity confirmation. The concentration of dsRNA was measured by NanoDrop 2000 spectrophotometer (Thermo Fisher Scientific) and adjusted to a final concentration of 2  $\mu$ g/ $\mu$ l in PBS. The double-stranded green fluorescent protein (GFP) gene was generated using a similar procedure and employed as a control to exclude the effect of dsRNA.

##### 2.7.2. In vivo RNAi

Chinese mitten crabs were divided into three groups (A, B and C) each containing five crabs. Group A was used as the experimental group for RNAi analysis. The amount of dsRNA infected into each crab was proportional to its body weight. Crabs in Group B were injected with an equal volume of dsGFP as negative controls, and Group C were untreated (UT). DsRNA injections were repeated 24 h after the first dsRNA injection, and bacterial stimulation (*S. aureus*) was performed 12 h after the second injection. *EsGPCR89* transcripts were measured by qRT-PCR at 12 h post-bacterial injection.  $\beta$ -actin was used as an internal control.

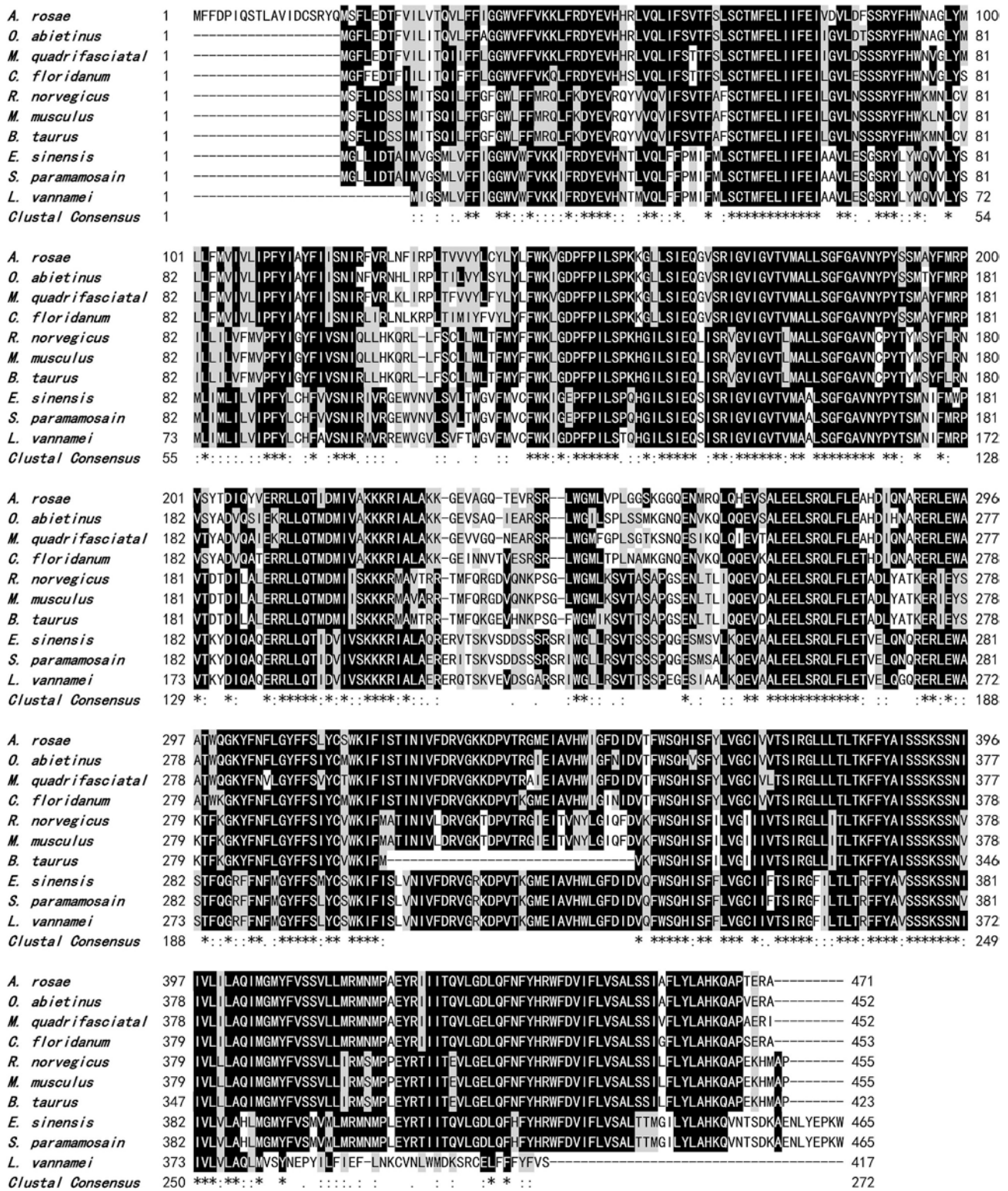


**Fig. 3.** Multiple alignment of *EsGPCR89* with *GPCR89* sequences from other species. Sequences and accession numbers of proteins used for alignment are as follows: *Athalia rosae* XP\_012253771.1, *Orussus abietinus* XP\_012277244.1, *Melipona quadrifasciata* KOX74220.1, *Copidosoma floridanum* XP\_014206094.1, *Rattus norvegicus* NP\_001132958.1, *Mus musculus* AAH10729.1, *Bos taurus* AAX46453.1, *Scylla paramamosain* ADG60269.1, *Litopenaeus vannamei* XP\_027237721.1. Single letter amino acid codes for conserved (identity = 100%), semi-conserved (≥75%) and variable (≥50%) residues are shaded black, grey and white, respectively.

**2.8. Expression of antimicrobial peptide (AMP) genes**

After bacterial infection as described in 2.2 and silencing of *EsGPCR89* as described in 2.7.2, total RNA was extracted and reverse transcription was performed. Expressions of AMPs in brain after

pathogen infection and expression after RNA interference were the measured by qRT-PCR. AMPs were selected according to previous publications, and their specific primers are listed in Table 1. The selected AMPs were anti-lipopolysaccharide factor (*EsALF1*) [39], anti-lipopolysaccharide factor 2 (*EsALF2*) [40], anti-lipopolysaccharide 3

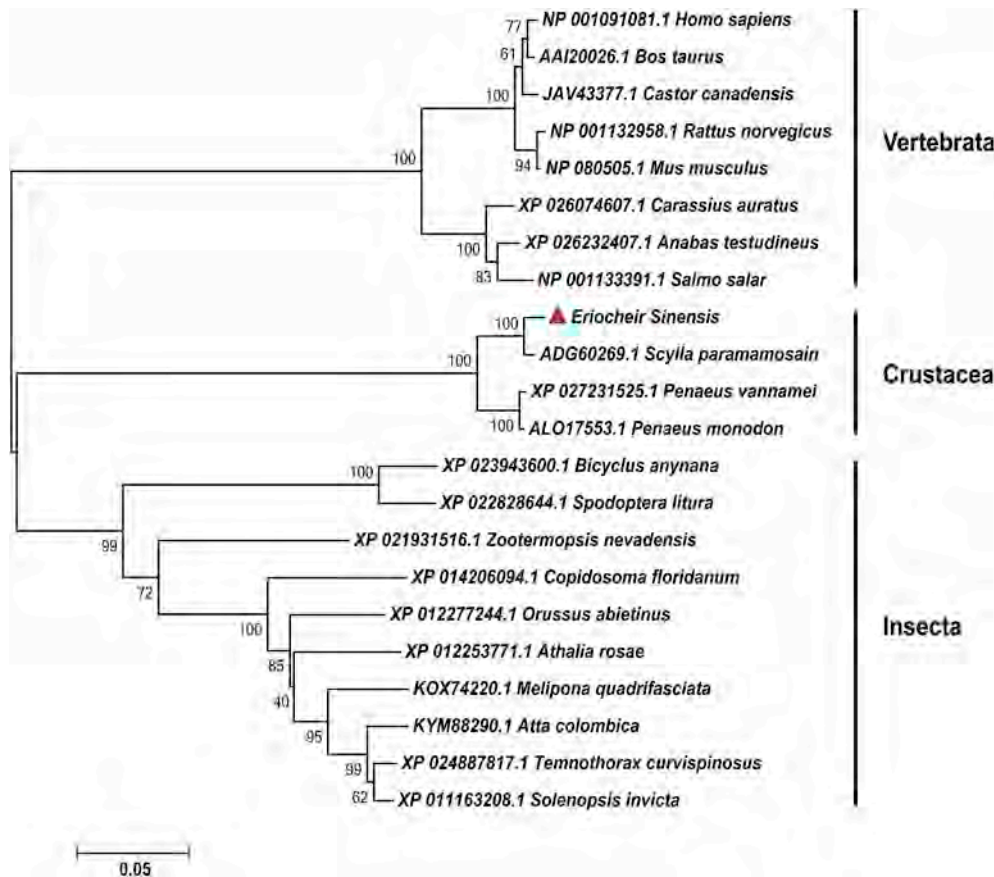


**Fig. 4. Neighbour-joining (NJ) phylogenetic analysis of EsGPCR89 proteins.** The NJ phylogenetic tree of GPCRs from various species was constructed using the MEGA 7.0 sequence analysis tool. The red triangle (▲) indicates EsGPCR89, while sequences and accession numbers from other organisms are as follows: *Scylla paramamosain* ADG60269.1, *Rattus norvegicus* NP\_001132958.1, *Mus musculus* NP\_080505.1, *Bos taurus* AAI20026.1, *Litopenaeus vannamei* XP\_027231525.1, *Homo sapiens* NP\_001091081.1, *Athalia rosae* XP\_012253771.1, *Melipona quadrifasciata* KOX74220.1, *Penaeus monodon* ALO17553.1, *Orussus abietinus* XP\_012277244.1, *Solenopsis invicta* XP\_011163208.1, *Temnothorax curvispinosus* XP\_024887817.1, *Atta colombica* KYM88290.1, *Zootermopsis nevadensis* XP\_021931516.1, *Spodoptera litura* XP\_022828644.1, *Bicyclus anynana* XP\_023943600.1, *Salmo salar* NP\_001133391.1, *Carassius auratus* XP\_026074607.1, *Anabas testudineus* XP\_026232407.1, *Castor canadensis* JAV43377.1, *Copidosoma floridanum* XP\_014206094.1. For interpretation of the references to colour in this figure legend, the reader is referred to the online version of this article. (For interpretation of the references to colour in this figure legend, the reader is referred to the Web version of this article.)

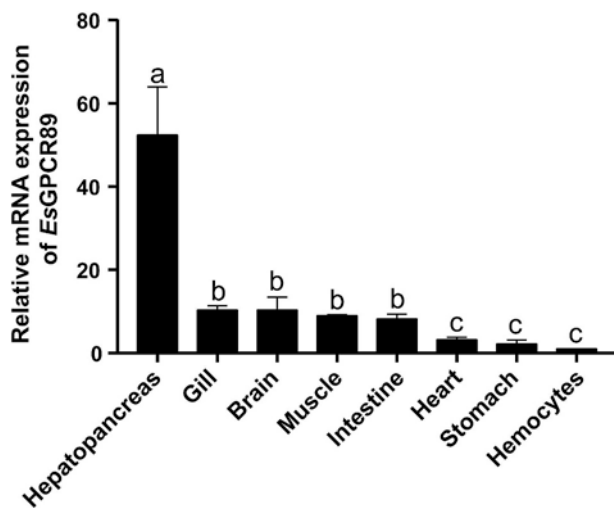


**Fig. 5. Tissue-specific expression patterns of EsGPCR89.** Real-time PCR analysis of EsGPCR89 transcription in different tissues of unchallenged *E. sinensis*.  $\beta$ -actin was used as an internal control. Data are presented as means  $\pm$  SD from triplicate experiments. The same letters above bars indicate that expression levels are not significantly different, while different letters indicate significant differences ( $p < 0.05$ ).

(*EsALF3*) [41], crustin (*EsCrus1*) [42], *EsCrus2* [43], a double WAP domain-containing protein (*EsDWD1*) [44] and lysozyme (*EsLys*) [45]. All experiments were performed three times.

**2.9. Immunisation assay**

Immunisation assays were based on RNAi. Three groups of healthy

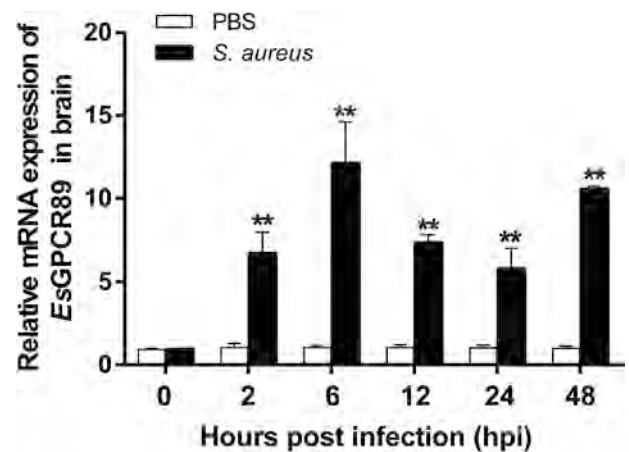
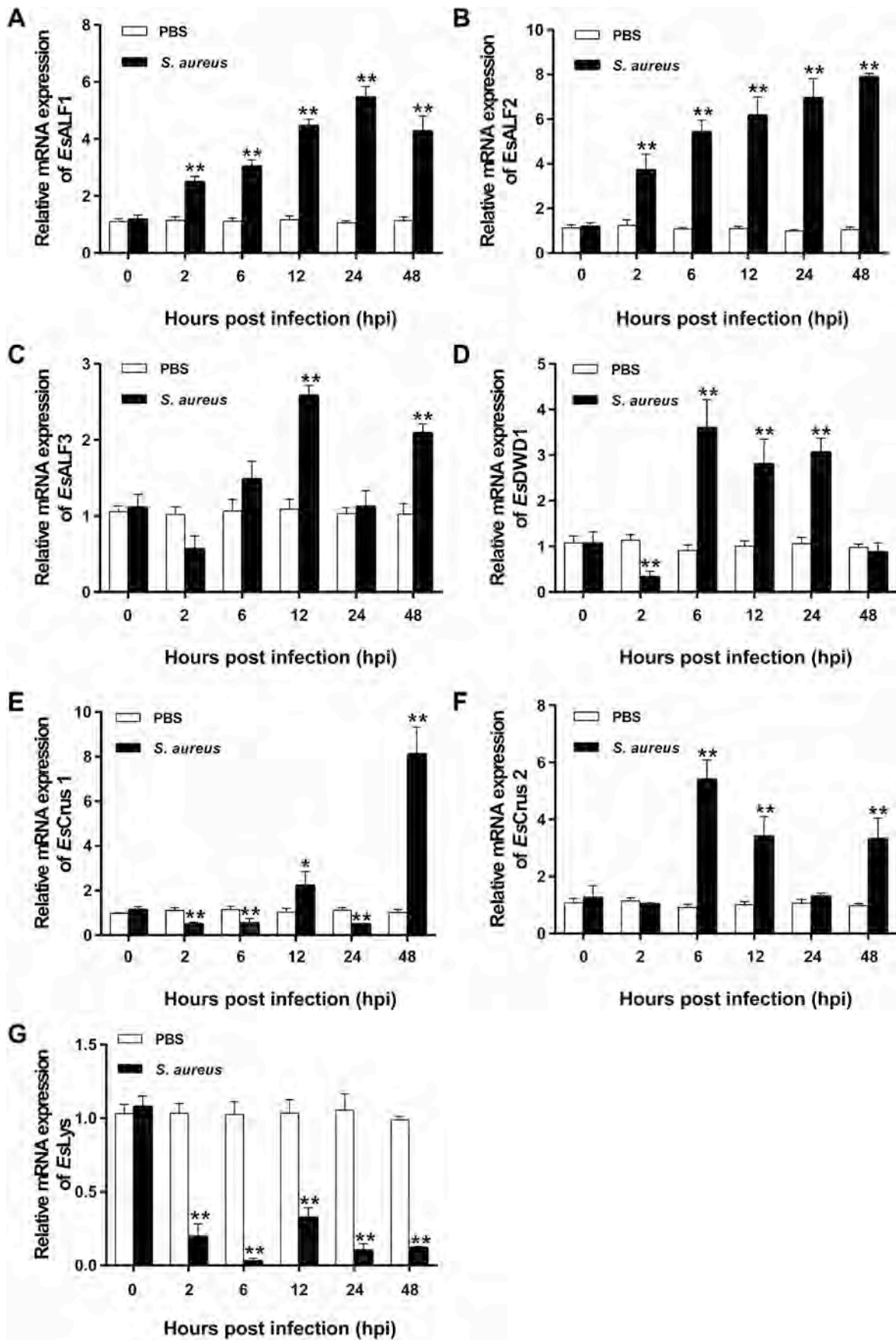


**Fig. 6. Expression pattern of EsGPCR89 in brain.** Expression profile of EsGPCR89 mRNA after *S. aureus* injection in brain. PBS was used as a negative control, and qRT-PCR was performed to examine the expression of EsGPCR89 in each sample, with  $\beta$ -actin as an internal reference gene. The x-axis represents the time post-injection, and the y-axis represents the corresponding relative expression level. All assays were performed three times and data were analysed by multiple t-tests ( $*p < 0.05$ ,  $**p < 0.01$  compared with controls).

Chinese mitten crabs were selected, and two groups (B and C) were respectively injected with dsGPF or dsEsGPCR89, while Group A remained untreated as controls. RNAi assays were performed according to 2.7.2. Crabs treated with dsGPF or dsEsGPCR89 were then infected with *S. aureus*, hemolymph was extracted from the three groups and centrifuged to separate serum, hemocytes were used to test the efficiency of interference, and serum was filtered with a microporous filter membrane and injected into other healthy crabs. Brains were collected 12 h



(caption on next page)

**Fig. 7. Expression of AMPs in brain.** qRT-PCR Analysis of the relative expression of (A) *EsALF1*, (B) *EsALF2*, (C) *EsALF3*, (D) *EsDWD1*, (E) *EsCrus-1*, (F) *EsCrus-2* and (G) *EsLys* in brain after *S. aureus* challenge for 0, 2, 6, 12, 24 and 48 h. Expression was normalised using PBS-injected crabs as negative controls, and the  $\beta$ -actin as an internal reference gene. The x-axis indicates the time post-injection, and the y-axis represents the relative expression levels of different AMPs. Three technical replicates were performed with at least three crabs for each sample, and results are presented as the mean  $\pm$  SD. Statistical significance is indicated by asterisks (\*\* $p < 0.01$ , \* $p < 0.05$ ).

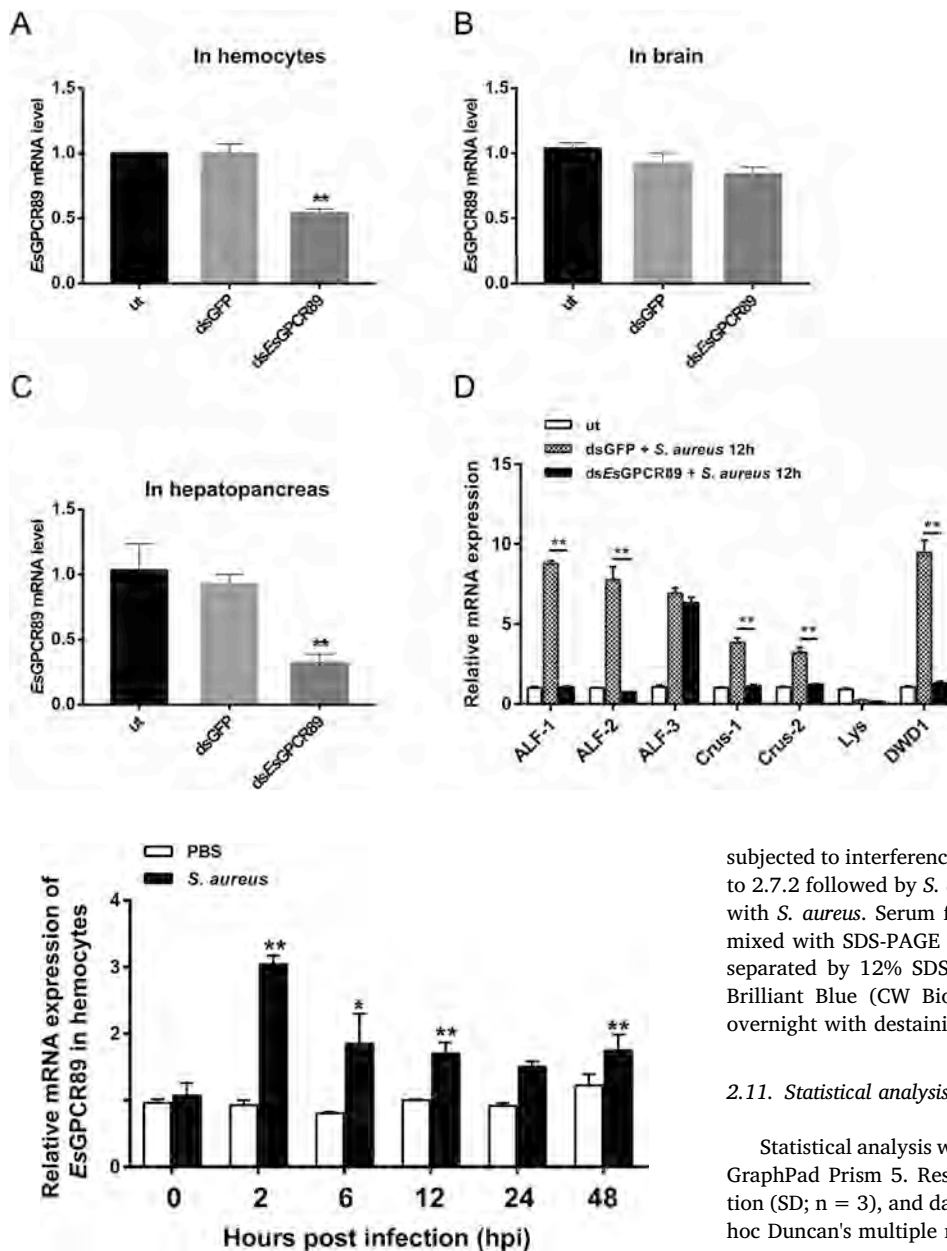


**Fig. 9. Expression of *EsGPCR89* in hemocytes after bacterial infection *in vivo*.** Temporal *EsGPCR89* mRNA expression in hemocytes following *S. aureus* infection *in vivo*.  $\beta$ -actin was used as an internal control for all experiments. Values were normalised using the Livak ( $2^{-\Delta\Delta Ct}$ ) method, and data are displayed as means  $\pm$  SD from three independent replicates. Statistical significance between control and treated groups is indicated by asterisks (\*\* $p < 0.01$ , \* $p < 0.05$ ).

later, total RNA was extracted, and transcription levels of AMP genes were calculated by qRT-PCR.

#### 2.10. Polyacrylamide gel electrophoresis (SDS-PAGE)

Crabs were divided into three groups, Groups A and B were

**Fig. 8. Expression of AMPs in brain following RNAi silencing of *EsGPCR89*.** The efficiency of RNAi silencing of *EsGPCR89* in (A) hemocytes, (B) brain and (C) hepatopancreas was determined. The expression level of *EsGPCR89* in the dsGFP group served as a control. (D) AMP mRNA expression levels in the brains of *EsGPCR89*-silenced crabs following *S. aureus* infection. AMP expression levels in the brains of the dsGFP group served as controls. Bars represent mean values from three repeats (\*\* $p < 0.01$ ).

subjected to interference assays with dsGFP and ds*EsGPCR89* according to 2.7.2 followed by *S. aureus* infection, and Group C was only injected with *S. aureus*. Serum from the three groups was collected 12 h later, mixed with SDS-PAGE loading buffer, heated at 100 °C for 8 min, and separated by 12% SDS-PAGE. Proteins were stained with Coomassie Brilliant Blue (CW Biotech, China) at 37 °C for 2 h, and destained overnight with destaining solution (CW Biotech).

#### 2.11. Statistical analysis

Statistical analysis was executed using SPSS software (ver. 11.0) and GraphPad Prism 5. Results are expressed as mean  $\pm$  standard deviation (SD;  $n = 3$ ), and data were subjected to one-way ANOVA and post-hoc Duncan's multiple range tests. Significance was set at  $p < 0.05$ .

### 3. Results

#### 3.1. Identification and bioinformatics analysis of *EsGPCR89*

The full-length of *EsGPCR89* sequence (GenBank accession number MN057664) is 2277 bp and contains a 1398 bp ORF encoding a 465 amino acid (aa) polypeptide, a 114 bp 5' untranslated region (UTR), and a 765 bp 3' UTR (Fig. 1). *EsGPCR89* appears to include four transmembrane regions residues 4–26, 38–60, 75–97 and 109–128), a Golgi pH regulator domain (GPHR\_N domain, aa 141–208), a low-complexity region (aa 221–229) and an abscisic acid (ABA) GPCR domain (aa 279–449) according to SMART software prediction (Fig. 2A). Transmembrane regions were also predicted using the TMHMM Server (Fig. 2B). Multiple sequence alignment revealed relatively high

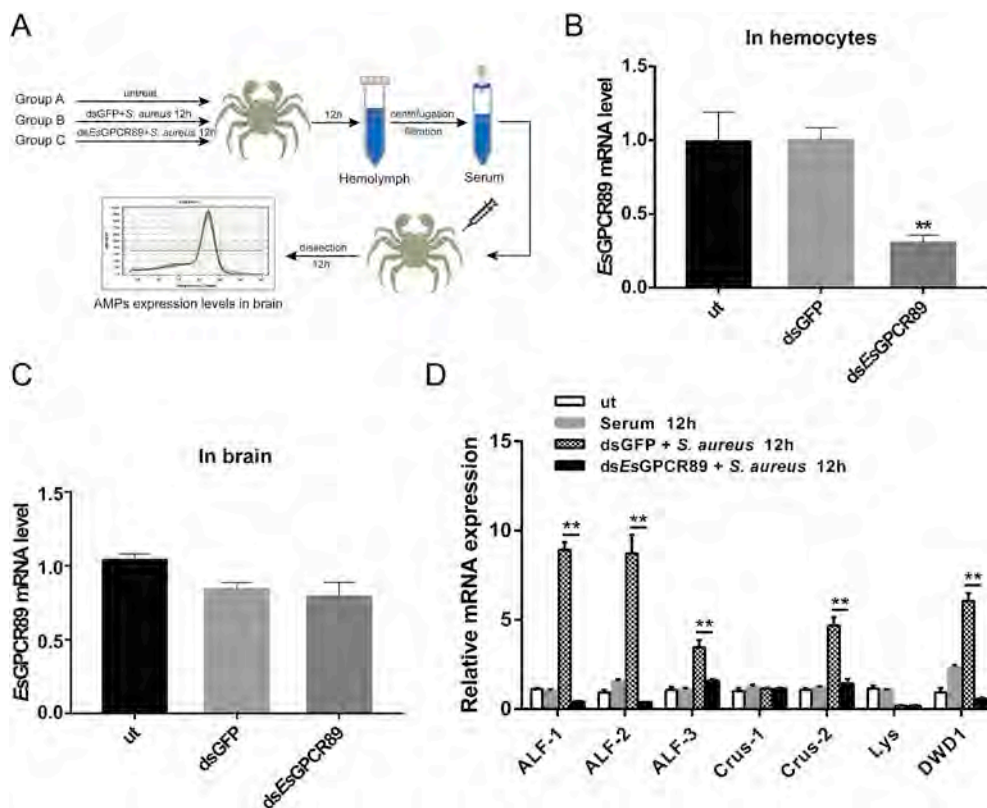


**Fig. 10. Expression of AMPs in brain analysed by immunisation assays.** (A) Flow chart of the immunisation assay. The effect of dsRNA silencing on transcription of *EsGPCR89* in (B) hemocytes and (C) brain was measured by qRT-PCR. (D) At 12 h after infecting treated crabs with *S. aureus*, immunised serum was collected from the three groups (healthy, dsGFP and ds*EsGPCR89*), and injected into other healthy crabs. Brains were collected 12 h later and transcription of AMPs was quantified. The dsGFP group was used as a control, and data were analysed by t-tests (\*\* $p < 0.01$ ).

sequence conservation with homologs in other species (Fig. 3) and evolutionary relationships were investigated by phylogenetic analysis of GPCR89 aa sequences from insects, crustaceans, mammals and other organisms obtained from GenBank. *EsGPCR89* proteins are separated into three groups (Vertebrata, Crustacea and Insecta), and the NJ tree therefore corresponds to traditional taxonomic classification, with closer relatedness to crustaceans than vertebrates (Fig. 4).

### 3.2. Expression profiles of *EsGPCR89* in different tissues

We used qRT-PCR to analyse the relative expression levels of *EsGPCR89* in selected tissues. The results showed that *EsGPCR89* was widely distributed in various tissues in crabs, and abundant in the hepatopancreas, followed by immune organs such as gill and intestine, as well as brain and muscle. However, expression levels in heart, stomach and hemocytes were relatively low (Fig. 5).

### 3.3. Expression profiles of *EsGPCR89* in brain following *S. aureus* infection

Relative expression levels of *EsGPCR89* in brain after injection with *S. aureus* were measured by qRT-PCR. At 2 h after bacterial infection, expression of *EsGPCR89* was up-regulated 6.5-fold ( $p < 0.01$ ), and remained elevated at 48 h, but there were no significant changes in *EsGPCR89* expression in the control group (Fig. 6). This result revealed a potential immune function for *EsGPCR89* in brain.

### 3.4. Regulation of AMP gene expression in crab brain

In order to explore the immune response in brain, we examined expression of AMP genes following bacterial infection. qRT-PCR was used to measure mRNA levels of immune-related genes *EsALF1*, *EsALF2*, *EsALF3*, *EsLys*, *EsCrus1*, *EsCrus2* and *EsDWD1* (Fig. 7). Expression levels of *EsALF1*, *EsALF2*, *EsALF3*, *EsCrus-1*, *EsCrus2* and *EsDWD1* were markedly up-regulated after *S. aureus* infection (Fig. 7A–F), and up-regulation of *EsALF1* and *EsALF2* (Fig. 7A and B)

lasted from 2 to 48 h, indicating higher sensitivity to *S. aureus*. By contrast, expression of *EsLys* (Fig. 7G) was significantly down-regulated following infection. The above results indicate that the brain may be protected against bacterial threat by up-regulating AMPs.

### 3.5. *EsGPCR89* RNAi in vivo

To investigate the effects of *EsGPCR89* on regulating the expression of immune-related genes in brain immunity, an *in vivo* *EsGPCR89* RNAi assay was performed. The interference efficiency was detected at 12 h after secondary injection of dsRNA. *EsGPCR89* expression was significantly ( $p < 0.01$ ) silenced in experimental but not control (untreated and dsGFP) group hemocytes (Fig. 8A), especially in hepatopancreas (silencing rate up to 80%; Fig. 8C). However, there were no significant changes in *EsGPCR89* expression in brain after silencing (Fig. 8B).

We also examined mRNA levels of immune-related genes in *EsGPCR89*-interference crab brains after *S. aureus* challenge. The results showed that *EsALF1*, *EsALF2*, *EsCrus1*, *EsCrus2* and *EsDWD1* were significantly down-regulated following *S. aureus* challenge (Fig. 8D).

### 3.6. Expression profiles of *EsGPCR89* in hemocytes following *S. aureus* infection

We next focused on whether the *EsGPCR89* gene in hemocytes, vital to immunity in crustaceans, could respond to bacterial infection. Transcription of *EsGPCR89* in hemocytes after infection by *S. aureus* was measured at different time points by qRT-PCR. The results showed that expression of *EsGPCR89* was increased at 2 h (~3-fold,  $p < 0.01$ ) then decreased to ~1.5-fold thereafter (Fig. 9).

### 3.7. Regulation of brain AMPs in hemocytes by *EsGPCR89*

The possible roles of *EsGPCR89* in regulating brain AMPs in hemocytes were investigated using RNAi-based gene silencing technology

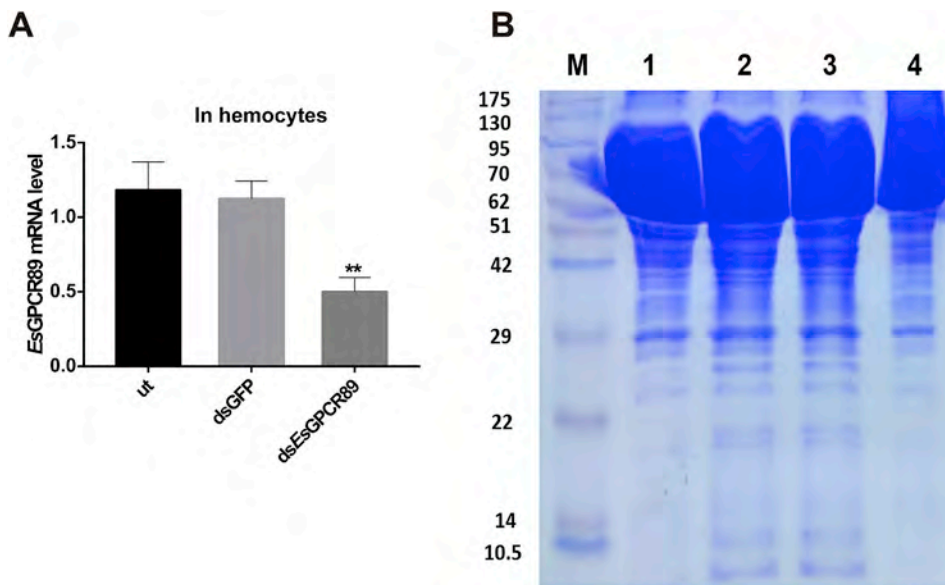


**Fig. 11.** Expression of proteins in serum following RNAi silencing of *EsGPCR89*. The efficiency of *EsGPCR89* silencing by RNAi in (A) hemocytes was determined by qRT-PCR. Assays were performed three times and analysed by t-tests (\*\* $p < 0.01$ ). (B) Expression of proteins in serum after RNAi analysed by 12% SDS-PAGE. Lane M, protein markers from 10.5 to 175 kDa. Lane 1, proteins in healthy crab serum; lane 2, proteins in serum after *S. aureus* infection; lane 3, proteins in serum after dsGFP injection at 12 h following *S. aureus* infection; lane 4, proteins in serum from *EsGPCR89*-silenced crabs at 12 h after infection with *S. aureus*.

and followed by bacterial challenge. *EsGPCR89* silencing was performed by injecting with *EsGPCR89*-dsRNA twice over a 24 h interval. *EsGPCR89* silencing resulted in decreased *EsGPCR89* expression in hemocytes (Fig. 10A), but no remarkable changes in brain tissue (Fig. 10B). In immunisation assays, mRNA levels of AMP genes in crabs injected with untreated serum showed no significant differences from control crabs. However, distinct differences were apparent between dsGFP-treated and ds*EsGPCR89*-silenced serum groups for gene expression levels of cerebral *EsALF1*, *EsALF2*, *EsALF3*, *EsCrus2* and *EsDWD1* ( $p < 0.01$ ; Fig. 10C). This result indicates that *EsGPCR89* in hemocytes is likely associated with the expression of cerebral AMPs in response to *S. aureus* infection.

Furthermore, differences in serum components between different treatment groups were revealed by SDS-PAGE. Compared with serum from ds*EsGPCR89*-silenced hemocytes that exhibited an interference efficiency of ~50% (Fig. 11A), serum from ds*EsGPCR89*-silenced crabs followed by *S. aureus* infection (lane 4) was clearly different from crabs pre-injected with dsGFP (lane 3), specifically in terms of proteins with a molecular weight of ~10 and 20 kDa (Fig. 11B). Meanwhile, serum from the *S. aureus*-challenged negative control group (lane 2) did not show any detectable differences compared with the dsGFP-treated group.

#### 4. Discussion

In the present study, GPCR gene was cloned from *E. Sinensis*, and characterisation revealed an immune function. The identified gene was previously recorded as GPCR89 (GenBank [ADG60269.1](#) for *Scylla paramamosain*) and shares homology with vertebrate GPCR89, hence we named it *EsGPCR89*. We first obtained the ORF encoding a 465 aa protein with a predicted molecular weight of 53.94 kDa, and two functional domains (GPHR\_N domain and ABA\_GPCR domain) were predicted by SMART analysis. GPHR\_N shares homology with the N-terminal 5TM regions of Golgi pH regulator proteins found in eukaryotes involved in transport of newly synthesised proteins from the Golgi to the plasma membrane [46], and these proteins are targeted to the Golgi [47]. Members of the ABA\_GPCR domain family are present in eukaryotes, and they have also been studied in plants [48], but their functions in crustaceans are poorly understood. Multiple sequence alignment revealed high sequence conservation for the GPHR domain in *EsGPCR89* [46], and evolutionary relationships were in accordance with traditional taxonomic classification.

Tissue-specific expression pattern analysis revealed a broad distribution for the *EsGPCR89* gene in Chinese mitten crab, with high expression in hepatopancreas, intestine and gill, indicating an immune function [18]. *EsGPCR89* was also relatively highly expressed in brain. According to previous publications, members of the GPCR superfamily are widely distributed cell membrane receptors found in metazoans [17], and signal transduction is the main physiological function in vertebrates [49]. The nervous system is reported to respond to various types of nonspecific stimulation, and it works in close conjunction with the immune system to regulate host defences [50–52]. In *Caenorhabditis elegans*, a GPCR named *NPR-1* (Neuropeptide Receptor) involved in neural circuit function suppresses innate immune responses [53]. In addition, some mammal GPCRs such as chemokine receptors are involved in immune responses [54], and chemokines may be the primary signal transmitter system in brain tissue [55]. Inspired by our results and previous research, we decided to explore the immune function of *EsGPCR89* in brain, and the relationship between neural and immune systems. We also examined expression patterns of *EsGPCR89* in brain at different times after *S. aureus* infection *in vivo*. The results showed that *EsGPCR89* was up-regulated in brain, indicating a potential role in cerebral immunity.

Invertebrates have evolved physiological mechanisms to defend against invading pathogens, including activating the expression of innate immune-related genes such as AMPs [56]. The brain also has its own immune responses, and we explored AMP gene expression following *S. aureus* infection. The results showed that all immune response genes detected were up-regulated except *EsLys*, indicating production of AMPs upon triggering of immune responses.

Thus, we investigated whether up-regulation of *EsGPCR89* after pathogen infection was related to the regulation of AMPs in the brain using *in vivo* *EsGPCR89* interference assays. The results confirmed that the *EsGPCR89* gene was successfully silenced in hepatopancreas and hemocytes, but unexpectedly, interference failed in brain, possibly due to the blood-brain barrier formed by glial cells in avascular invertebrates that protects against direct exposure to hazardous substances [57,58]. Next, we examined the transcriptional levels of cerebral AMPs after various treatments. We found that mRNA levels of *EsALF1*, *EsALF2*, *EsCrus1*, *EsCrus2* and *EsDWD1* were significantly down-regulated compared with controls. This suggests that the observed decrease in the expression of AMPs in brain might be due to *EsGPCR89* silencing in other tissues in crab. We subsequently measured *EsGPCR89* expression in hemocytes following *S. aureus* injection by

qRT-PCR, and observed up-regulation at 2 h, which supports this hypothesis.

Hemocytes are important in various cellular and humoral immune reactions processes including phagocytosis, encapsulation, and releasing antibiotic substances [59]. The invertebrate cardiovascular system is an open vascular system in which hemolymph bathes tissues and substances exchange directly between cells and hemolymph [60]. Based on the results described above, we could infer that increasing the expression of *EsGPCR89* in hemocytes after bacterial infection might be associated with activation of cerebral AMP gene transcription. In order to investigate the connection between the brain and hemocytes, we performed immunisation experiments. Compared with the experimental group, increased expression of some AMP genes in the dsGFP group indicates that some effectors are generated by signalling pathways involving *EsGPCR89* in hemocytes, and they may then trigger expression of various AMP genes to protect brain tissue. Expression of *EsCrus1* and *EsLys* was not significantly altered, suggesting they may be activated in other ways.

GPCRs transmit special signals to the cell through G proteins to regulate diverse cellular and physiological events and accumulating evidence demonstrate that GPCRs play an active role in transcriptional regulation [61]. Studies have shown that GPCR-mediated transcriptional regulation focuses on the activation of nuclear factor (NF) - $\kappa$ B, a transcription factor that profoundly affected leukocyte function and inflammatory processes [62,63]. In addition, GPCRs has also been shown to regulate insulin secretion [64] and one of the adhesion GPCR called brain-specific angiogenesis inhibitor 1 (*BALI*) could mediate macrophage reactive oxygen species (ROS) production and microbicidal activity against Gram-negative bacteria [65]. Therefore, to confirm our hypothesis that *EsGPCR89* expression in hemocytes might stimulate transcription of effector molecules that affect cerebral immune responses, SDS-PAGE was performed. The results demonstrated the generation of effect factors, consistent with our hypothesis. However, the exact effectors and the specific pathways stimulated require further investigation.

In summary, we isolated the full-length *EsGPCR89* gene in Chinese mitten crab, and tissue expression patterns revealed broad tissue expression. The results of bacterial infection assays indicate a putative immune function in brain, and this was further corroborated by RNAi silencing. In addition, immunisation experiments and SDS-PAGE further verified the linkage between hemocytes and the brain. Thus, infection by *S. aureus* appears to up-regulate *EsGPCR89* in hemocytes, and this stimulates the transcription and release of undetermined effectors that activate cerebral AMP gene expression to protect the brain. GPCRs are an important class of cell membrane surface receptors. This large number of GPCRs enable cells to respond to a variety of sensory inputs such as odorants, light, lipids, ions, amines and nucleotides, as well as signal peptides and proteins such as hormones, morphogens and neurotransmitters [66]. Hence, GPCRs are well-established targets for many drugs. For example, past results of serotonin (*5-HT*) in the brain provide new targets for drug development in major depression [32]. Therefore, we speculated that the effectors from hemocytes after pathogen stimulation were to regulate the expression of antimicrobial peptides in the brain by binding to a GPCR receptor on the surface of the brain. Based on the results of our research and the existing literature, we will focus on exploring the mechanism by which GPCRs regulate the production of secreted proteins by hemocytes and the immune-related signal transduction mechanisms in the brain. Our results provide a basis for future studies on the linkage between immune and nervous systems in invertebrates.

## Acknowledgements

This work was supported by the National Natural Science Foundation of China (Grant No. 31602189 and 31672639), the State Key Laboratory of Estuarine and Coastal Research, and the Laboratory

of Invertebrate Immunological Defense and Reproductive Biology, School of Life Science, East China Normal University, Shanghai, China.

## References

- [1] S. Akira, S. Uematsu, O. Takeuchi, Pathogen recognition and innate immunity, *Cell* 124 (4) (2006) 783–801.
- [2] K. Azumi, R. De Santis, A. De Tomaso, I. Rigoutsos, F. Yoshizaki, M.R. Pinto, R. Marino, K. Shida, M. Ikeda, M. Ikeda, M. Arai, Y. Inoue, T. Shimizu, N. Satoh, D.S. Rokhsar, L. Du Pasquier, M. Kasahara, M. Satake, M. Nonaka, Genomic analysis of immunity in a Urochordate and the emergence of the vertebrate immune system: "waiting for Godot", *Immunogenetics* 55 (8) (2003) 570–581.
- [3] L. Du Pasquier, Speculations on the origin of the vertebrate immune system, *Immunol. Lett.* 92 (1–2) (2004) 3–9.
- [4] D. Cooper, I. Eleftherianos, Memory and specificity in the insect immune system: current perspectives and future challenges, *Front. Immunol.* 8 (2017) 539.
- [5] J. Kurtz, K. Franz, Innate defence: evidence for memory in invertebrate immunity, *Nature* 425 (6953) (2003) 37–38.
- [6] R. Medzhitov, C.A. Janeway Jr., Decoding the patterns of self and nonself by the innate immune system, *Science* 296 (5566) (2002) 298–300.
- [7] D. Hultmark, Drosophila immunity: paths and patterns, *Curr. Opin. Immunol.* 15 (1) (2003) 12–19.
- [8] C. Dostert, E. Jouanguy, P. Irving, L. Troxler, D. Galiana-Arnoux, C. Hetru, J.A. Hoffmann, J.L. Imler, The Jak-STAT signaling pathway is required but not sufficient for the antiviral response of drosophila, *Nat. Immunol.* 6 (9) (2005) 946–953.
- [9] L. Cerenius, K. Soderhall, The prophenoloxidase-activating system in invertebrates, *Immunol. Rev.* 198 (2004) 116–126.
- [10] J.A. Hoffmann, J.M. Reichhart, Drosophila innate immunity: an evolutionary perspective, *Nat. Immunol.* 3 (2) (2002) 121–126.
- [11] S.V. Balandin, T.V. Ovchinnikova, Antimicrobial peptides of invertebrates. Part 1. structure, biosynthesis, and evolution, *Russ. J. Bioorganic Chem.* 42 (3) (2016) 229–248.
- [12] I. Galea, I. Bechmann, V.H. Perry, What is immune privilege (not)? *Trends Immunol.* 28 (1) (2007) 12–18.
- [13] M.D. Nguyen, J.P. Julien, S. Rivest, Innate immunity: the missing link in neuroprotection and neurodegeneration? *Nat. Rev. Neurosci.* 3 (3) (2002) 216–227.
- [14] S. Rivest, Regulation of innate immune responses in the brain, *Nat. Rev. Immunol.* 9 (6) (2009) 429–439.
- [15] A.D. Howard, G. McAllister, S.D. Feighner, Q. Liu, R.P. Nargund, L.H. Van der Ploeg, A.A. Patchett, Orphan G-protein-coupled receptors and natural ligand discovery, *Trends Pharmacol. Sci.* 22 (3) (2001) 132–140.
- [16] K.J. Nordstrom, M. Sallman Almen, M.M. Edstam, R. Fredriksson, H.B. Schioth, Independent HHsearch, Needleman–Wunsch-based, and motif analyses reveal the overall hierarchy for most of the G protein-coupled receptor families, *Mol. Biol. Evol.* 28 (9) (2011) 2471–2480.
- [17] M.C. Lagerstrom, H.B. Schioth, Structural diversity of G protein-coupled receptors and significance for drug discovery, *Nat. Rev. Drug Discov.* 7 (4) (2008) 339–357.
- [18] H. Jiang, Y.M. Cai, L.Q. Chen, X.W. Zhang, S.N. Hu, Q. Wang, Functional annotation and analysis of expressed sequence tags from the hepatopancreas of mitten crab (*Eriocheir sinensis*), *Mar. Biotechnol.* 11 (3) (2009) 317–326.
- [19] A. Kohyama-Koganeya, Y.J. Kim, M. Miura, Y. Hirabayashi, A Drosophila orphan G protein-coupled receptor BOSS functions as a glucose-responding receptor: loss of boss causes abnormal energy metabolism, *Proc. Natl. Acad. Sci. U.S.A.* 105 (40) (2008) 15328–15333.
- [20] W. Song, R. Ranjan, K. Dawson-Scully, P. Bronk, L. Marin, L. Seroude, Y.J. Lin, Z. Nie, H.L. Atwood, S. Benzer, K.E. Zinsmaier, Presynaptic regulation of neurotransmission in Drosophila by the g protein-coupled receptor methuselah, *Neuron* 36 (1) (2002) 105–119.
- [21] D.P. Srivastava, E.J. Yu, K. Kennedy, H. Chatwin, V. Reale, M. Hamon, T. Smith, P.D. Evans, Rapid, nongenomic responses to ecdysteroids and catecholamines mediated by a novel Drosophila G-protein-coupled receptor, *J. Neurosci.* 25 (26) (2005) 6145–6155.
- [22] R.T. Birse, E.C. Johnson, P.H. Taghert, D.R. Nassel, Widely distributed Drosophila G-protein-coupled receptor (CG7887) is activated by endogenous tachykinin-related peptides, *J. Neurobiol.* 66 (1) (2006) 33–46.
- [23] T.E. Hebert, M. Bouvier, Structural and functional aspects of G protein-coupled receptor oligomerization, *Biochem. Cell Biol.* 76 (1) (1998) 1–11.
- [24] R.P. Metpally, R. Sowdhamini, Genome wide survey of G protein-coupled receptors in Tetraodon nigroviridis, *BMC Evol. Biol.* 5 (2005) 41.
- [25] A.J. Kooistra, R. Leurs, I.J. de Esch, C. de Graaf, From three-dimensional GPCR structure to rational ligand discovery, *Adv. Exp. Med. Biol.* 796 (2014) 129–157.
- [26] W.K. Kroeze, D.J. Sheffler, B.L. Roth, G-protein-coupled receptors at a glance, *J. Cell Sci.* 116 (Pt 24) (2003) 4867–4869.
- [27] F.B. Bang, A bacterial disease of *Limulus polyphemus*, *Bull. Johns Hopkins Hosp.* 98 (5) (1956) 325–351.
- [28] S. Kurata, S. Ariki, S. Kawabata, Recognition of glucogens and activation of immune responses in Drosophila and horseshoe crab innate immunity, *Immunobiology* 211 (4) (2006) 237–249.
- [29] J.R. Powell, D.H. Kim, F.M. Ausubel, The G protein-coupled receptor FSHR-1 is required for the Caenorhabditis elegans innate immune response, *Proc. Natl. Acad. Sci. U.S.A.* 106 (8) (2009) 2782–2787.
- [30] C. Dong, P. Zhang, A putative G protein-coupled receptor involved in innate immune defense of *Procambarus clarkii* against bacterial infection, *Comp. Biochem.*

- Physiol. Mol. Integr. Physiol. 161 (2) (2012) 95–101.
- [31] Y. Jia, B. Yang, W. Dong, Z. Liu, Z. Lv, Z. Jia, L. Qiu, L. Wang, L. Song, A serotonin receptor (Cg5-HTR-1) mediating immune response in oyster *Crassostrea gigas*, *Dev. Comp. Immunol.* 82 (2018) 83–93.
- [32] D.O. Borruto-Escuela, J. Carlsson, P. Ambrogini, M. Narvaez, K. Wydra, A.O. Tarakanov, X. Li, C. Millon, L. Ferraro, R. Cuppini, S. Tanganelli, F. Liu, M. Filip, Z. Diaz-Cabiale, K. Fuxe, Understanding the role of GPCR heteroreceptor complexes in modulating the brain networks in health and disease, *Front. Cell. Neurosci.* 11 (2017) 37.
- [33] T. Schwabe, R.J. Bainton, R.D. Fetter, U. Heberlein, U. Gaul, GPCR signaling is required for blood-brain barrier formation in *Drosophila*, *Cell* 123 (1) (2005) 133–144.
- [34] R. Daneman, B.A. Barres, The blood-brain barrier—lessons from moody flies, *Cell* 123 (1) (2005) 9–12.
- [35] H.H. Huss, Control of indigenous pathogenic bacteria in seafood, *Food Control* 8 (2) (1997) 91–98.
- [36] V.J. Smith, K. Soderhall, Induction of degranulation and lysis of haemocytes in the freshwater crayfish, *Astacus astacus* by components of the prophenoloxidase activating system in vitro, *Cell Tissue Res.* 233 (2) (1983) 295–303.
- [37] K.J. Livak, T.D. Schmittgen, Analysis of relative gene expression data using real-time quantitative PCR and the 2(-Delta Delta C(T)) Method, *Methods* 25 (4) (2001) 402–408.
- [38] H. Liu, P. Jiravanichpaisal, L. Cerenius, B.L. Lee, I. Soderhall, K. Soderhall, Phenoloxidase is an important component of the defense against *Aeromonas hydrophila* Infection in a crustacean, *Pacifastacus leniusculus*, *J. Biol. Chem.* 282 (46) (2007) 33593–33598.
- [39] C. Li, J. Zhao, L. Song, C. Mu, H. Zhang, Y. Gai, L. Qiu, Y. Yu, D. Ni, K. Xing, Molecular cloning, genomic organization and functional analysis of an anti-lipoplysaccharide factor from Chinese mitten crab *Eriocheir sinensis*, *Dev. Comp. Immunol.* 32 (7) (2008) 784–794.
- [40] Y. Zhang, L. Wang, L. Wang, J. Yang, Y. Gai, L. Qiu, L. Song, The second anti-lipoplysaccharide factor (EsALF-2) with antimicrobial activity from *Eriocheir sinensis*, *Dev. Comp. Immunol.* 34 (9) (2010) 945–952.
- [41] W. Leilei, A new anti-lipoplysaccharide factor (EsALF-3) from *Eriocheir sinensis* with antimicrobial activity, *Afr. J. Biotechnol.* 10 (77) (2011).
- [42] C. Mu, P. Zheng, J. Zhao, L. Wang, H. Zhang, L. Qiu, Y. Gai, L. Song, Molecular characterization and expression of a crustin-like gene from Chinese mitten crab, *Eriocheir sinensis*, *Dev. Comp. Immunol.* 34 (7) (2010) 734–740.
- [43] C. Mu, P. Zheng, J. Zhao, L. Wang, L. Qiu, H. Zhang, Y. Gai, L. Song, A novel type III crustin (CrusEs2) identified from Chinese mitten crab *Eriocheir sinensis*, *Fish Shellfish Immunol.* 31 (1) (2011) 142–147.
- [44] S. Li, X.K. Jin, X.N. Guo, A.Q. Yu, M.H. Wu, S.J. Tan, Y.T. Zhu, W.W. Li, Q. Wang, A double WAP domain-containing protein Es-DWD1 from *Eriocheir sinensis* exhibits antimicrobial and proteinase inhibitory activities, *PLoS One* 8 (8) (2013) e73563.
- [45] L. Pan, F. Yue, J. Miao, L. Zhang, J. Li, Molecular cloning and characterization of a novel c-type lysozyme gene in swimming crab *Portunus trituberculatus*, *Fish Shellfish Immunol.* 29 (2) (2010) 286–292.
- [46] Y. Maeda, T. Ide, M. Koike, Y. Uchiyama, T. Kinoshita, GPHR is a novel anion channel critical for acidification and functions of the Golgi apparatus, *Nat. Cell Biol.* 10 (10) (2008) 1135–1145.
- [47] J.C. Edwards, C.R. Kahl, Chloride channels of intracellular membranes, *FEBS Lett.* 584 (10) (2010) 2102–2111.
- [48] S. Pandey, D.C. Nelson, S.M. Assmann, Two novel GPCR-type G proteins are abscisic acid receptors in *Arabidopsis*, *Cell* 136 (1) (2009) 136–148.
- [49] D.M. Rosenbaum, S.G. Rasmussen, B.K. Kobilka, The structure and function of G-protein-coupled receptors, *Nature* 459 (7245) (2009) 356–363.
- [50] E.M. Sternberg, Neural regulation of innate immunity: a coordinated nonspecific host response to pathogens, *Nat. Rev. Immunol.* 6 (4) (2006) 318–328.
- [51] J. Andersson, The inflammatory reflex—introduction, *J. Intern. Med.* 257 (2) (2005) 122–125.
- [52] K.J. Tracey, The inflammatory reflex, *Nature* 420 (6917) (2002) 853–859.
- [53] K.L. Styer, V. Singh, E. Macosko, S.E. Steele, C.I. Bargmann, A. Aballay, Innate immunity in *Caenorhabditis elegans* is regulated by neurons expressing NPR-1/GPCR, *Science* 322 (5900) (2008) 460–464.
- [54] R.P. Metpally, R. Sowdhamini, Cross genome phylogenetic analysis of human and *Drosophila* G protein-coupled receptors: application to functional annotation of orphan receptors, *BMC Genomics* 6 (2005) 106.
- [55] M.W. Adler, T.J. Rogers, Are chemokines the third major system in the brain? *J. Leukoc. Biol.* 78 (6) (2005) 1204–1209.
- [56] O.E. Sorensen, N. Borregaard, A.M. Cole, Antimicrobial peptides in innate immune responses, *Contrib. Microbiol.* 15 (2008) 61–77.
- [57] A. Quaegebeur, I. Segura, P. Carmeliet, Pericytes: blood-brain barrier safeguards against neurodegeneration? *Neuron* 68 (3) (2010) 321–323.
- [58] N.J. Abbott, Dynamics of CNS barriers: evolution, differentiation, and modulation, *Cell. Mol. Neurobiol.* 25 (1) (2005) 5–23.
- [59] A.F. Rowley, A. Powell, Invertebrate immune systems specific, quasi-specific, or nonspecific? *J. Immunol.* 179 (11) (2007) 7209–7214.
- [60] C.L. Reiber, I.J. McGaw, A review of the “open” and “closed” circulatory systems: new terminology for complex invertebrate circulatory systems in light of current findings, *Int. J. Zool.* 2009 (2009) 1–8.
- [61] R.D. Ye, Regulation of nuclear factor kappaB activation by G-protein-coupled receptors, *J. Leukoc. Biol.* 70 (6) (2001) 839–848.
- [62] P.A. Baeuerle, T. Henkel, Function and activation of NF-kappa B in the immune system, *Annu. Rev. Immunol.* 12 (1994) 141–179.
- [63] S. Ghosh, M.J. May, E.B. Kopp, NF-kappa B and Rel proteins: evolutionarily conserved mediators of immune responses, *Annu. Rev. Immunol.* 16 (1998) 225–260.
- [64] J.B. Regard, H. Kataoka, D.A. Cano, E. Camerer, L. Yin, Y.W. Zheng, T.S. Scanlan, M. Hebrok, S.R. Coughlin, Probing cell type-specific functions of Gi in vivo identifies GPCR regulators of insulin secretion, *J. Clin. Investig.* 117 (12) (2007) 4034–4043.
- [65] E.A. Billings, C.S. Lee, K.A. Owen, R.S. D’Souza, K.S. Ravichandran, J.E. Casanova, The adhesion GPCR Bai1 mediates macrophage ROS production and microbicidal activity against Gram-negative bacteria, *Sci. Signal.* 9 (413) (2016) ra14.
- [66] M.J. Marinissen, J.S. Gutkind, G-protein-coupled receptors and signaling networks: emerging paradigms, *Trends Pharmacol. Sci.* 22 (7) (2001) 368–376.